PERGAMON

International Journal of Heat and Mass Transfer 44 (2001) 111–119

International Journal of HEAT and MASS TRANSFER

www.elsevier.com/locate/ijhmt

Porosity formation in axi-symmetric castings produced by counter-pressure casting method

I.H. Katzarov[a,*], Y.B. Arsov[a], P. Stoyanov[b], T. Zeuner[b], A. Buehrig-Polaczek[b], P.R. Sahm[b]

[a]*Institute of Metal Science, Bulgarian Academy of Sciences, 67, Sipchenski prohod str., 1574 Sofia, Bulgaria*
[b]*Giesserei-Institut, RWTH, Intzestr., 52072 Aachen, Germany*

Received 22 February 2000

Abstract

We propose a method for simultaneous treatment of heat and mass transfer processes and porosity formation of castings produced by Counter Pressure Casting (CPC) method. The method enables us to account for the influence of the CPC parameters on the mechanical properties of the casting. Numerical results and comparison with experimental data are given for an axis-symmetric casting (hemisphere with constant wall thickness). © 2000 Elsevier Science Ltd. All rights reserved.

1. Introduction

The aim of the present work was the creation of an algorithm for simulation of the porosity formation in axis-symmetric castings produced by Counter Pressure Casting (CPC) method. The important features of CPC method are the possibility for controlling the form filling time and the temperature in the mould, and improving the feeding of the two-phase region by applying pressure in the melt during solidification. The criteria functions, such as Niyama criteria, which describe the location of the likely porosity, cannot be used for evaluation of the influence of the pressure on the process of porosity formation. We have developed a program module for numerical calculation of the formation of porosity defects (both gaseous and shrinkage porosity), which can account for the influence of Counter Pressure Casting process parameters. Within this approach the porosity formation is described by a non-linear system of differential equations including the constitutional equations of the alloy, the equation describing the interdendritic feeding, and mass and gas content conservation equations.

2. Mathematical formulation of porosity formation problem

The porosity problem is solved jointly with the problem for heat and mass transfer. A method is propose in [1] for treating the heat and mass transfer problem in a boundary-fitted coordinate system. The equations describing heat and mass transfer were written and numerically solved in a covariant way in a specially designed Finite Differences Method (FDM)-grid, obtained after generating of a family of surfaces congruent to the boundaries of the region. With a special choice of the components G_{ij} of the metric tensor at the nodes, the surfaces can be considered as coordinate

* Corresponding author. Tel.: +359-2-7142-363; fax: +359-2-703-207.
E-mail address: ivo@ims.bas.bg (I.H. Katzarov).

0017-9310/01/$ - see front matter
PII: S0017-9310(00)00085-5

surfaces of a boundary-fitted coordinate system. In this coordinate system the problems of heat and mass transfer, related to the casting formation, can be treated simultaneously (Fig. 1).

The equations of heat and mass transfer are obtained in a covariant way in order to account for the effects of boundary curvature and nonstationarity. The Navier–Stokes equation is derived from the conservation laws in the Riemannian space:

$$\text{(a) mass} \qquad \left(1/\sqrt{G}\right)\partial_t\left(\sqrt{G}\rho\right) + \nabla\cdot(\rho\mathbf{u}) = 0$$

(b) momentum

$$\rho(\partial_t\mathbf{u} + \mathbf{u}\cdot\nabla\mathbf{u} + 2\Gamma\cdot\mathbf{u}) - \nabla\sigma = \rho F \tag{1}$$

where $\mathbf{u}$ is the velocity; ρ, specific density; Γ^k_{ij}, affine connection coefficients; σ^{ij}, stress tensor and F, the external force density.

The heat problem is solved in two regions — the cavity of the mould and the mould itself. In the mould the heat conductivity equation is:

$$c\rho\partial_t T = \lambda\Delta T \tag{2}$$

In the cavity of filling the heat equation is considered also in two regions — the one with frozen metal where Eq. (2) is solved and the other with molten metal where the heat equation becomes

$$\rho(c + L\partial_T f_S)\partial_t T = \lambda\Delta T - \rho c\mathbf{u}\cdot\nabla T \tag{3}$$

Here $u(t,\mathbf{r})$ is the velocity obtained from Eq. (1); c, heat capacity; λ, heat conductivity and L, the latent heat of crystallisation. The crystallisation is described by the method of equivalent heat capacity

$$c_E = c - L\partial_T f_S$$

To solve the above equation the relationship between the solid fraction f_S and temperature T is needed. One limit of the relationship is obtained from Sheil's equation, which ignores the solid diffusion as

$$f_S = 1 - \left(\frac{T - T_m}{T_L - T_m}\right)^{\frac{1}{k-1}}$$

The model describing the porosity formation is based on the pressure drop evaluation in the interdendritic liquid. The local pressure P in the two-phased region is calculated from a system of two differential equations — continuity equation and Darcy law. The continuity equation

$$\left(\frac{\rho_S}{\rho_L} - 1\right)\frac{\partial f_L}{\partial t} - \nabla\cdot(f_L\mathbf{u}) + \frac{\partial f_P}{\partial t} = 0 \tag{4}$$

indicates that the shrinkage during the solidification (first term) is compensated by the interdendritic flow

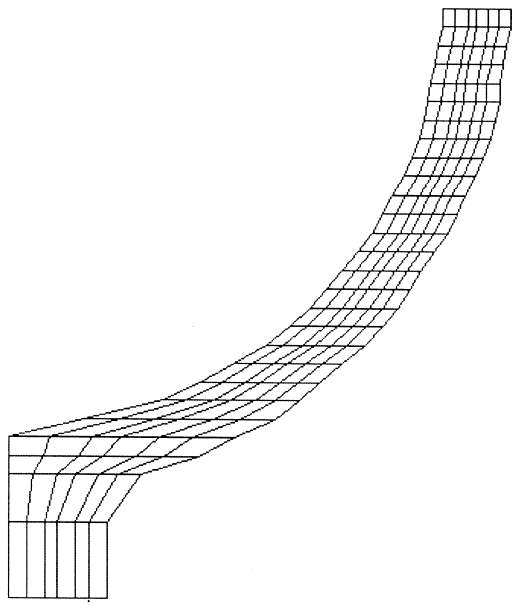

Fig. 1. Boundary-fitted coordinate system used for simultaneous treatment of the problems of heat and mass transfer.

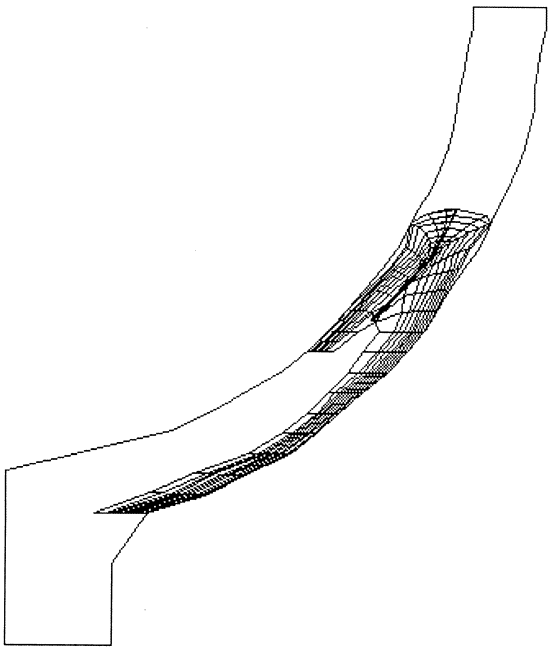

Fig. 2. Local boundary-fitted coordinate system generated over the two-phase region.

(second term) and the growth of porosity f_P [2]. Darcy's law

$$\mathbf{u} = -\frac{k_0}{\nu f_L}(\nabla P + \rho \mathbf{g}) \tag{5}$$

describes the interdendritic flow. The permeability k_0 in Eq. (5) is calculated from the liquid fraction f_L and the dendrite cell size d following Blake–Kozeney equation

$$k_0 = \frac{f_L^3 d^2}{180(1-f_L)^2}$$

The combination of microstructure simulation and of casting process simulation leads to conflict, due to the considerable dimensional difference between these two physical realities. The grid used for obtaining the numerical solution of the heat and mass transfer problem is too coarse for the description of the interdendritic mass diffusion in the mushy zone. In the present article the differential equations describing the processes of porosity formation are written and solved in a local coordinate system, generated over the two-phase region (Fig. 2). The coordinate surfaces are the isotherms, defined by the equation

$$T(\xi) = \text{const}$$

and the integral lines of the temperature gradients field given by

$$\frac{\mathrm{d}x^i}{\mathrm{d}\eta} = \nabla_i T(\mathbf{x}(\xi,\eta)) \tag{6}$$

With this choice of the coordinate lines the local coordinate system is fitted to the boundaries of the two-phase region. An additional advantage is that the coordinate system is orthogonal. The components of the metric tensor are obtained in the form

$$g_{\xi\xi} = g(\partial/\partial\xi, \partial/\partial\xi) = \left(\sum_{i=1}^{2}\frac{\mathrm{d}x^i}{\mathrm{d}\xi}\frac{\mathrm{d}x^i}{\mathrm{d}\xi}\right)^{1/2}$$

$$g_{\eta\eta} = g(\partial/\partial\eta, \partial/\partial\eta) = \left(\sum_{i=1}^{2}\frac{\mathrm{d}x^i}{\mathrm{d}\eta}\frac{\mathrm{d}x^i}{\mathrm{d}\eta}\right)^{1/2}$$

$$= \left(\sum_{i=1}^{2}\nabla_i T\cdot\nabla_i T\right)^{1/2} \tag{7}$$

Since the geometry of the mushy zone is non-stationary the local coordinate system is updated at each time step.

After substituting the velocity of the interdendritic mass feeding, described by the Darcy's law (5), into the continuity equation (4) the following equation describing the local pressure in the mushy zone is obtained

$$\mathbf{A}\Delta P + \mathbf{B}\cdot\nabla P + \mathbf{C} = 0 \tag{8}$$

where

$$\mathbf{A} = \frac{k_0}{\nu};\quad \mathbf{B} = \frac{3-f_L}{f_L(1-f_L)}\nabla f_L;$$

$$\mathbf{C} = \left(\frac{\rho_S}{\rho_L} - 1\right)\frac{\partial f_L}{\partial t} + \frac{\partial f_P}{\partial t} + \frac{\rho\mathbf{g}\cdot\nabla k_0}{\nu}.$$

In the local coordinate system with metric equation (7), Eq. (8) is written in the form

$$\left(g^{\xi\xi}P_{,\xi\xi} + g^{\eta\eta}P_{,\eta\eta}\right) + \left(\frac{\left(\sqrt{g}g^{\xi\xi}\right)_{,\xi}}{\sqrt{G}} + \frac{g^{\xi\xi}\mathbf{B}_\xi}{\mathbf{A}}\right)P_{,\xi} + \left(\frac{\left(\sqrt{g}g^{\eta\eta}\right)_{,\eta}}{\sqrt{g}} + \frac{g^{\eta\eta}\mathbf{B}_\eta}{\mathbf{A}}\right)P_{,\eta} + \frac{\mathbf{C}}{\mathbf{A}} = 0 \tag{9}$$

where

$$g = \det\left(g^{\alpha\beta}\right) = r^2 g^{\xi\xi} g^{\eta\eta}$$

We impose the following boundary conditions for Eq. (9):

(a) At the centreline and the mould wall of an axisymmetric casting

$$u_r = 0; \qquad \frac{\partial P}{\partial r} = 0$$

where u_r is the r-component of the velocity.

(b) Along the liquidus isotherm the pressure is equal to the pressure in the molten metal and the liquid metal flows to feed shrinkage:

$$u_\eta = \left(\frac{\rho_S}{\rho_L} - 1\right)u_L$$

where u_L is the liquid isotherm velocity

It is assumed that a gas pore is stable provided that the excess pressure in the gas is sufficient to overcome the surface tension when the gas phase has a radius that is small enough to fit in the interdendritic space [2,3]. The above requirement is expressed as

$$P_g - P = \frac{4\sigma_{GL}}{d} \tag{10}$$

where P_g is gas pressure; P, metal pressure and σ_{GL}, gas–liquid interfacial energy. Since the surface tension barrier to be overcome for the formation of gas pore within the secondary spacing would be much higher, d

is the primary dendrite cell size. The primary dendrite arm spacing depends on the thermal gradient in front of the dendrites G_L and the solidification rate R [4]

$$d = AG_L^a R^b$$

where A, a, b are constants.

When no porosity is formed, the metal pressure P is calculated from Eq. (9) by an implicit finite difference method. The interaction between the heat and pore formation problems takes place through the evolution of the two-phase region. Since the geometry of the mushy zone is non-stationary, the local coordinate system is updated at each time step.

The gas pressure is calculated from Eq. (10) assuming the diameter of porosity first being the dendrite cell size. A new amount of porosity is calculated from the conservation equation for gas content

$$[H_0] = (1 - f_L)[H_S] + f_L[H_L] + \alpha\frac{P_g f_P}{T} \tag{11}$$

which indicates that the initial hydrogen content $[H_0]$ is compensated by the amounts of hydrogen in the solid $[H_S]$, liquid $[H_L]$ and porosity fraction f_P [4,5]. Sievert's law expresses the hydrogen content in the solid and liquid

$$[H_S] = K_{SH}\sqrt{P_g}$$

$$[H_L] = K_{LH}\sqrt{P_g}$$

When the porosity is already formed, the metal and gas pressure are calculated from Eq. (9) using the amount of porosity before the current time Δt.

The procedure described above is repeated over each volume element in the two-phase region and at each time step.

3. Experiments and measurements of microstructure

A counter-pressure unit VP 400 at the Giesserei Institut, Aachen, was adapted for on-line monitoring and storage. Pressure sensors and thermocouples were connected with a measuring unit, consisting of a PC and specialised software (Fig. 3). This makes it possible to control the pressure in the furnace, the mould and mould chamber with an accuracy of nearly 0.05 bar and scanning rate of 9 Hz. Storage of the data allows the comparison between process parameters and casting, necessary for systematic experimentation.

Conventional NiCr–Ni thermocouples were installed for measuring the melting temperature and the temperature of the mould. The temperature was measured in the top half and the bottom half of the mould at a distance of 2 mm from the surface mould casting. Fig. 4 shows the location of the measurement sensors in the mould and the casting unit. Fig. 5 (test 56) shows the different pressure and temperature curves for a form-filling velocity of 0.02 bar/s and a form-fill-

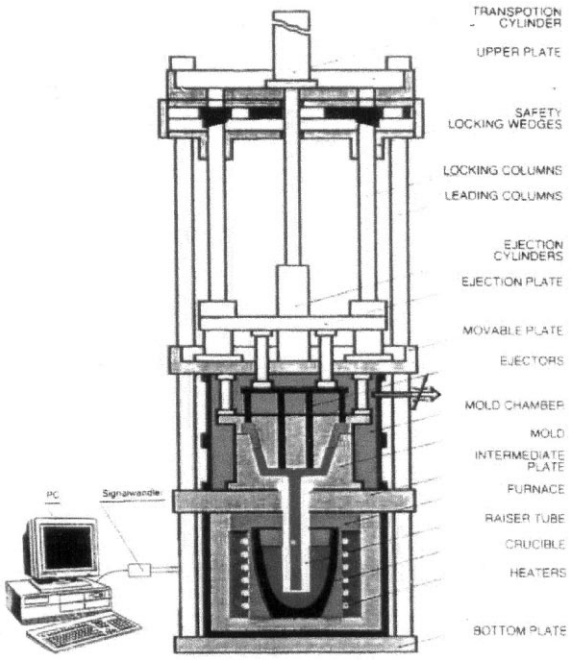

Fig. 3. Counter Pressure Casting unit with monitoring system.

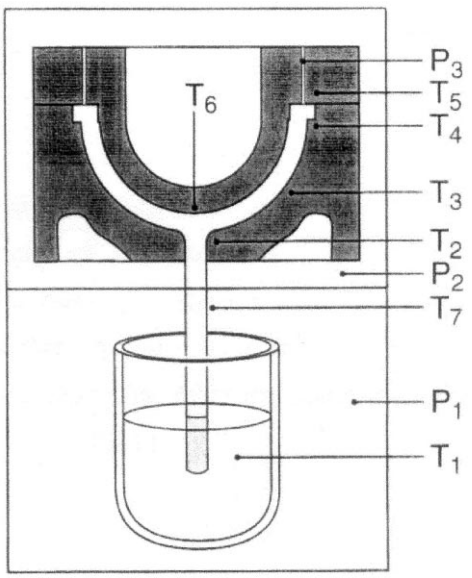

Fig. 4. Location of the measurement sensors in the mould and casting unit.

ing time of 20 s. In test 61 with a form-filling velocity of 0.07 bar/s the mould is filled after 10 s. After the filling the pressure difference continued for about 25 s.

To determine the porosity an image analyser (IBAS) measured the diameter of the pores and their total area to arrive at a quantitative description. Generally the level of pressure difference, the initial temperature distribution and the form-filling velocity have a considerable effect on the distribution of pores and density in different parts of the casting. In the top zone the cooling rate of the mould has more influence on the porosity than the pressure difference and the form-filling velocity. From 20–140 mm zone the porosity depends principally on the form-filling velocity. In the middle and bottom area of casting 56, the porosity in Fig. 6a, the amount of the measured porosity along the length of the casting is marked by $*$ symbols, is higher at lower rates of form-filling velocity than during increased form-filling velocity (casting 61, Fig. 6b) [6].

4. Numerical results and discussion

The porosity formation in the casting of demonstration part (hemisphere with constant wall thickness) was simulated using the present program module. The porosity formation in the casting of the demonstration part was simulated for form-filling times of about 10 and 20 s, which corresponded to experimental castings 56 and 61. The initial mould temperature distribution used in the calculations is obtained after simulating a number of successive test castings so that the temperature in the top half and the bottom half of the mould could be fitted to the temperature measured by the installed thermocouples. Fig. 6a and b show the distribution of measured ($*$ symbols) and calculated (solid lines) porosity over the length of the casting for the both form-filling times. Fig. 7a and b show the calculated distribution of pores in the casting for differential pressure of 3 bar. The comparison between the calculated and measured porosity on Fig. 6 shows satisfactory coincidence.

With the increasing form-filling velocity the porosity decreases. The calculated higher porosity both at lower rates of form-filling velocity and lower mold temperature can be explained by the occurrence of a wide mushy zone in the middle area in these cases. The obstructions to the interdendritic feeding increases and the porosity grow to compensate for the solidification shrinkage.

An important parameter that influences the porosity

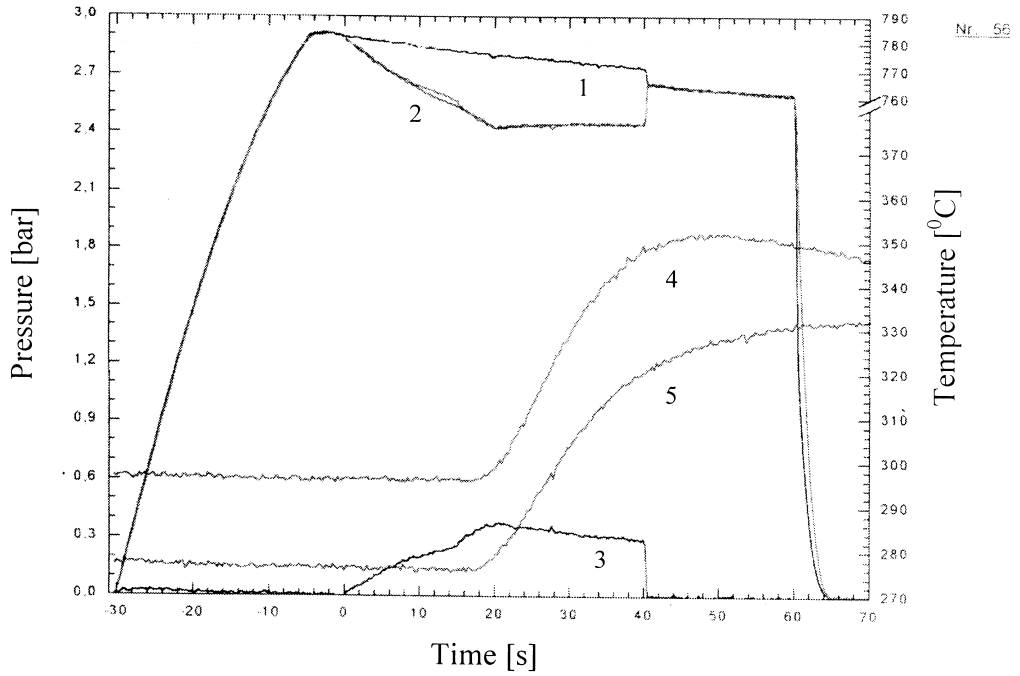

Fig. 5. Pressure and mould temperature curves for form-filling velocity of 0.02 bar/s: (1), pressure in the lower chamber, (2) pressure in the mould chamber, (3) differential pressure, (4) and (5) mould temperatures.

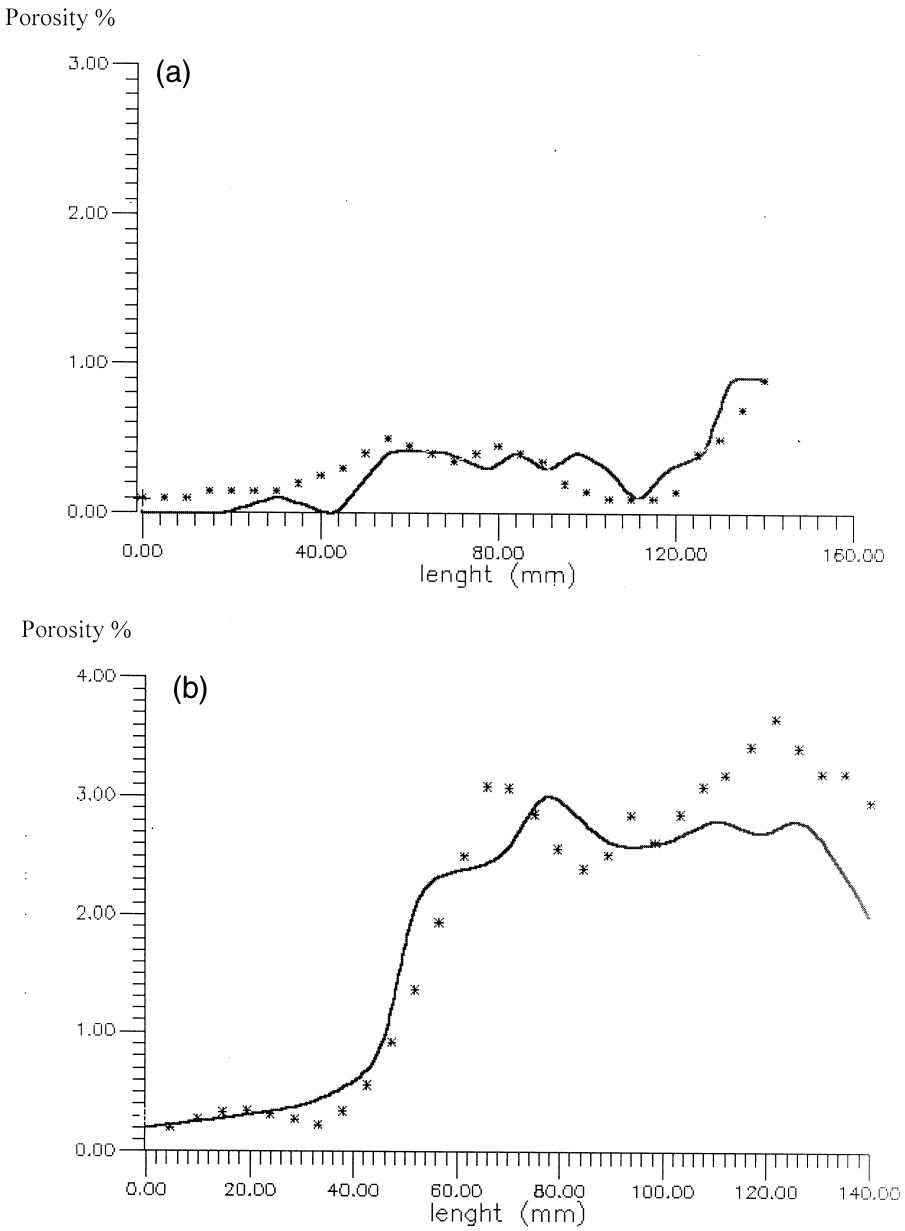

Fig. 6. Distribution of measured and calculated porosity over the length of the castings 56 and 61.

formation in a counter pressure casting unit is the differential pressure. The criteria functions, which describe the location of the likely porosity, cannot be used to evaluate the influence of the pressure on the porosity formation. This is possible by using the present program module. We investigated the influence of the pressure difference in two cases — with higher (test casting 61), and lower amount of pores (56). For both the cases, the porosity distribution is calculated by applying differential pressure of 3 bar (Fig. 7a and b) and 5 bar (Fig. 8a and b). It proves that the influence of the differential pressure is more valuable in the case when the width of the mushy zone remains smaller during the process of crystallisation. It is important to note that the study has not accounted for the fact that increasing differential pressure leads to an increasing cooling rate, which in turn influences the process of porosity formation.

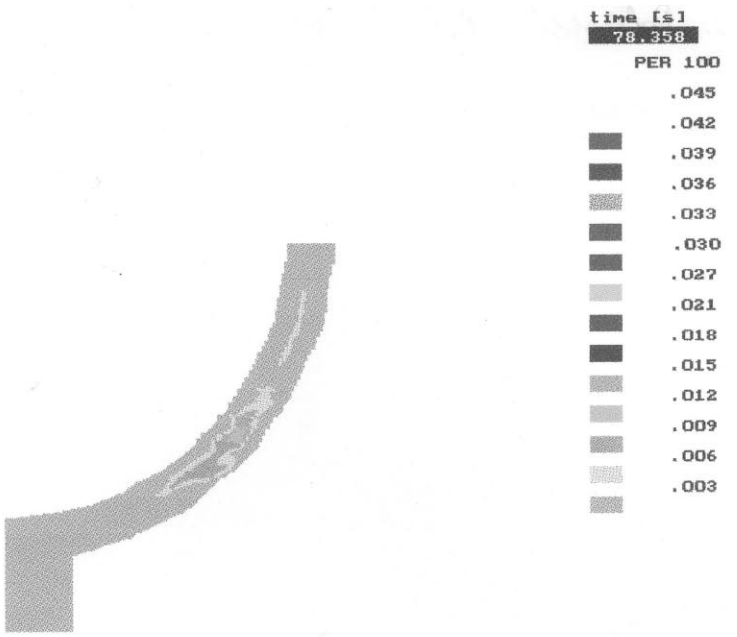

a

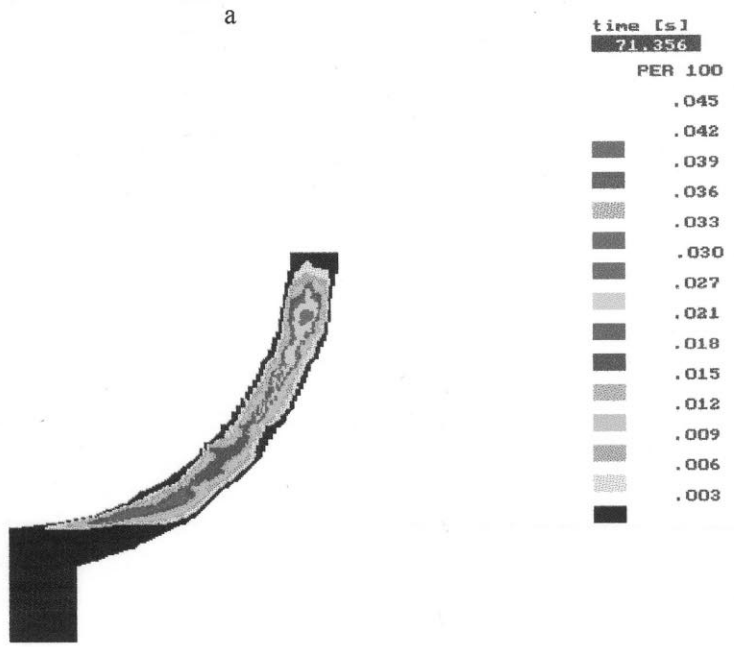

b

Fig. 7. Distribution of calculated porosity in the castings 56 and 61 for differential pressure of 3 bar.

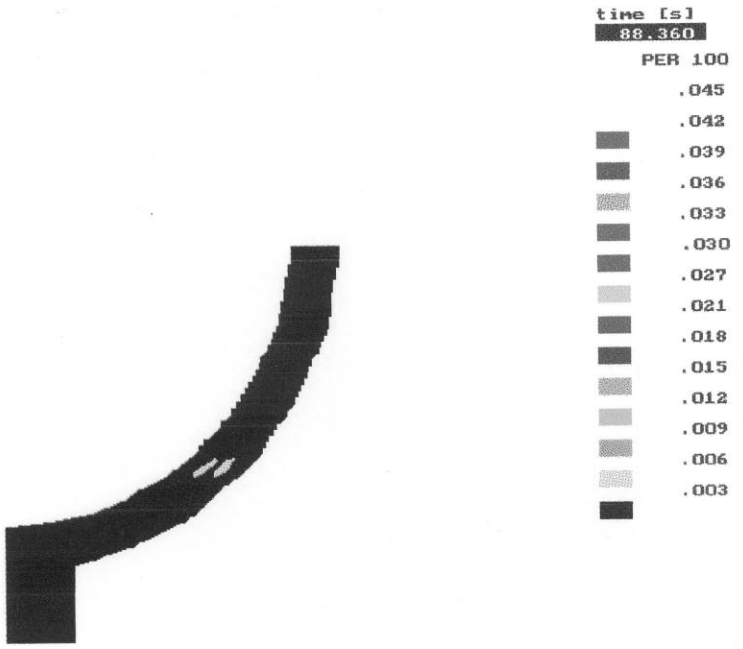

a

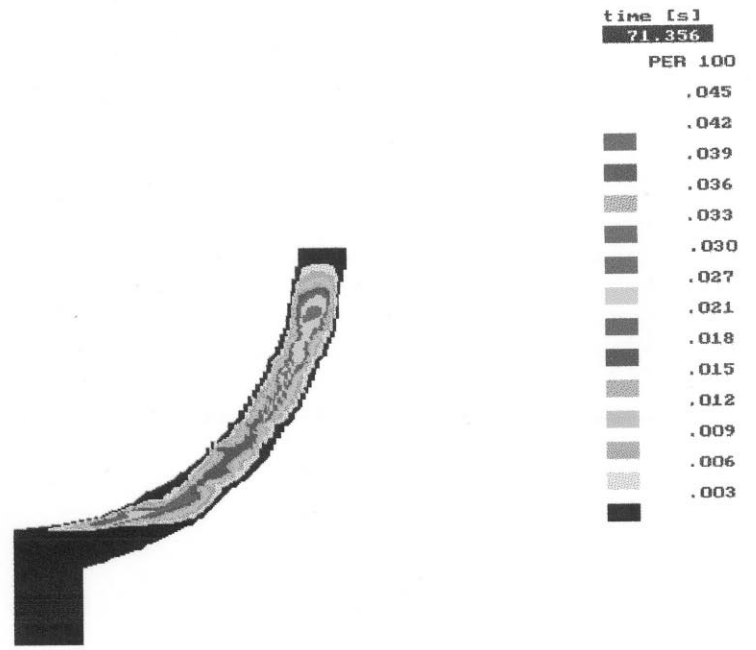

b

Fig. 8. Distribution of calculated porosity in the castings 56 and 61 for differential pressure of 5 bar.

References

[1] J.R. Popov, I.H. Katzarov, Mathematical modelling of heat and mass transfer problems in axially-symmetric forms with complicated geometry, Int. J. of Heat and Technology 8 (3/4) (1990) 60.

[2] K. Kubo, R. Pehlke, Mathematical modelling of porosity formation in solidification, Metall. Trans. B 16B (1985) 359.

[3] T.S. Pivonka, M.C. Flemings, Pore formation in solidification, Trans. Met. Soc. AIME 236 (1966) 1157.

[4] D.R. Pourier, K. Yeum, A. Maples, A thermodynamic prediction for microporosity formation in aluminium-rich Al–Cu alloys, Metall. Trans. A 18 (1987) 1979.

[5] V.K. Suri, A.J. Paul, HTD 218/AMD-139, Micro/macro scale phenomena in solidification, ASME, 1992.

[6] Casting of High Quality Cast Parts with Gaseous Counter-Pressure Casting Process Using Numerical Simulations — CIPA-CT94-0156, 1st Summary Progress Report, 01 March 95–31 Aug. 95.